AJNR

Volume-of-Interest Imaging of the Inner Ear in a Human Temporal Bone Specimen Using a Robot- Driven C-Arm Flat Panel Detector CT System

D. Kolditz, T. Struffert, Y. Kyriakou, A. Bozzato, A. Dörfler and W.A. Kalender

Volume-of-Interest Imaging of the Inner Ear in a Human Temporal Bone Specimen Using a Robot-Driven C-Arm Flat Panel Detector CT System

TECHNICAL NOTE

D. Kolditz
T. Struffert
Y. Kyriakou
A. Bozzato
A. Dörfler
W.A. Kalender

SUMMARY: VOI imaging can provide higher image quality at a reduced dose for a subregion. In this study with a robot-driven C-arm FDCT system, the goals were proof of feasibility for inner ear imaging, higher flexibility during data acquisition, and easier processing during reconstruction. First a low-dose OV scan was acquired allowing an orientation and enabling the selection of the VOI. The C-arm was then moved by the robotic system without a need for patient movement and the VOI was scanned with adapted parameters. Uncompromised artifact-free image quality was achieved by the 2-scan approach and the dose was reduced by 80%–90% in comparison with conventional MSCT and FPCT scans.

ABBREVIATIONS: DED = detector entrance dose; FPCT = flat panel detector CT; HD = high-dose; HU = Hounsfield unit; lp = line pairs; MSCT = multisection CT; OV = overview; SFOV = scan field of view; VOI = volume of interest

VOI imaging has been shown to be a promising approach for dose reduction in conebeam CT in recent years.[1-11] Besides dose reduction, this application also has some other potentials concerning image quality (eg, enabling higher resolution, lower noise, and scatter reduction).

A VOI imaging approach in C-arm-based FPCT[12,13] was developed and evaluated by the authors earlier.[11] Image-quality improvements and dose reduction were evaluated in simulations and measurements of dedicated phantoms. In the proposed method, 2 consecutive scans were obtained and combined: A low-dose OV scan of the whole patient cross-section provided OV information, and a high-dose VOI scan of a defined VOI provided detailed information for that VOI. Between the 2 scans, the patient was shifted by moving the treatment table according to the chosen VOI. The combination of both scans ensured higher image quality within the VOI than in a conventional scan, and the cumulative dose was reduced.

The main drawbacks of the proposed method were moving the patient between the 2 scans, which was necessary for the off-center VOI data acquisition, and the registration between the OV and VOI scans, which was necessary for the combination procedure. An image-based registration method, which used preliminary reconstructions, and a camera-based registration method, which used the information of an external optical tracking system, were proposed to determine the transformation.

In this work, we resolved these acquisition and registration problems by moving the C-arm instead of the patient and by using the C-arm coordinates of the robot for the combination. These updates make the proposed VOI technique easier to use in clinical application. To demonstrate the applicability and advantages for clinical examinations, we obtained measurements of phantoms and of a human inner ear specimen and compared them with reference scans. These investigations extended our phantom studies[11] and may highlight the applicability of FPCT for inner ear investigations.[14,15]

Materials and Methods

VOI Imaging in C-Arm-Based FPCT

The proposed VOI approach consists of 2 consecutive scans: an OV scan followed by a VOI scan. We briefly describe our VOI approach in the following 3 paragraphs.

OV Scan. The initial OV scan with the standard isocenter and a wide fan and z-collimation (Fig 1) serves to image a large volume (eg, the complete human head). This scan is obtained with a low dose, which can be achieved by a low number of projections, detector pixel binning, and a low radiation dose per projection. The reconstructed image has adequate image quality, allowing a general orientation. In this imaged volume, a second volume of arbitrary position, orientation, and size can be selected (eg, the human inner ear) to be imaged at higher image quality.

VOI Scan. A new isocenter is calculated to match the position, orientation, and size of the selected VOI, and the collimation is narrowed both in fan and z-direction to expose a smaller volume. Additionally, the spatial resolution can be increased by reducing the detector pixel binning and by using higher magnification. With the new parameters, a second scan around the new isocenter is obtained, often with a higher dose to provide lower noise. The increased dose can be achieved by a higher number of projections and a higher radiation dose per projection.

Combination of Data and Image Reconstruction. For the combination of the 2 scans, a forward projection of the reconstructed OV volume in the VOI scan geometry is performed. These artificial OV projection data are combined with the measured VOI data in the raw
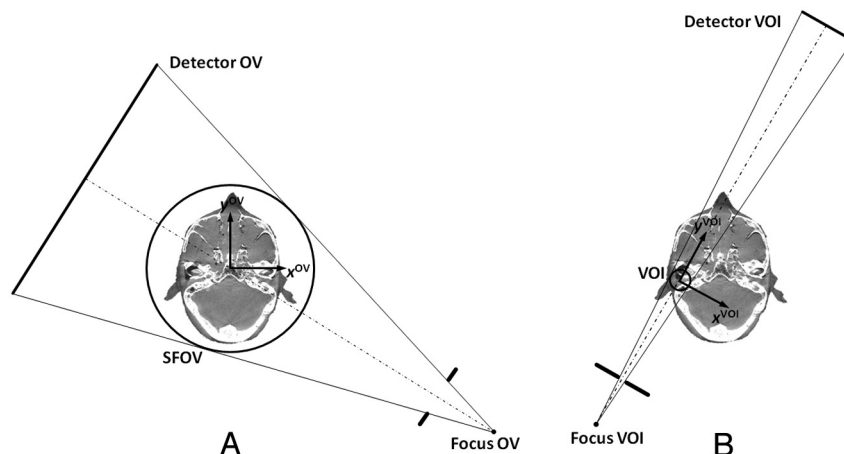
Fig 1. Definition of the C-arm FPCT geometry. *A*, OV scan with a wide open collimation and a large SFOV covering the complete patient cross-section. *B*, VOI scan with a narrowed collimation and a small SFOV only covering the region of interest.

data domain. The new set of combined data is reconstructed with the standard algorithm of Feldkamp et al.[16]

Specimen and Phantoms

Bar Pattern Phantom. A bar pattern phantom of 160 mm in diameter was used to investigate spatial resolution and image noise. The phantom consisted of water-equivalent material and contained high-contrast aluminum bar patterns representing resolution levels of 0.4–3.0 lp/mm with an increment of 0.2 lp/mm. Each bar pattern consisted of 6 aluminum bars arranged so that their distances equaled the bar thickness.

Temporal Bone Specimen. A temporal bone was dissected from the skull of a normal-hearing elderly patient who died from causes unrelated to ear or skull base disease. Written informed consent to use the body for research had been given. For the measurements, the specimen was inserted and fixed in a polymethylmethacrylate cylinder of 160 mm in diameter filled with water to mimic a patient setup.

FPCT Scanning

Measurements were performed with a robot-driven C-arm system (Artis zeego; Siemens Erlangen, Germany). This system is equipped with a flat detector of 40×30 cm^2 with 2480×1920 pixels and a pixel size of 154×154 μm^2. All scans were obtained in a circular partial scan with an angular range of 200°, which is typically used in C-arm–based FPCT.[17] The focal spot size was kept constant for all scans at 0.3 mm. The system magnification was also kept constant at 1.6 (1200 mm source-detector and 750 mm source-isocenter distance) because of system restrictions, though a higher magnification would further increase the spatial resolution.[1,11,18]

OV Scan. Before scanning, the bar pattern or the water cylinder, including the specimen, was centered in the SFOV. In the OV scan, 124 projections with a 4×4 pixel binning were acquired. The tube voltage was set to 70 kV, and the DED, to 0.10 μGy/projection. Reconstruction was performed with a smooth convolution kernel for a volume of $512 \times 512 \times 150$ voxels with a voxel size of $0.47 \times 0.47 \times 0.47$ mm^3. The VOI was a selected bar pattern or the inner ear, both of which were easily selected in the OV volume. The necessary offsets between the OV isocenter and the new VOI isocenter were determined.

VOI Scan. Before the VOI scan, the C-arm was moved and aligned along the selected VOI. This shift was manually performed by

using the system control because there is no automatic shift provided by the manufacturer in the current system version. However, the corresponding C-arm coordinates were directly read from the Artis zeego system. Neither the patient nor the treatment table was moved. For the VOI scan, 496 projections with a 2×2 pixel binning were acquired. Collimation was used to reduce the VOI size to 30 mm in diameter and 30 mm in length. The tube voltage was set to 70 kV, and the DED, to 3.60 μGy/projection. After the combination of OV and VOI data, the reconstruction was performed with a Shepp-Logan convolution kernel for the complete volume of $512 \times 512 \times 150$ voxels with a voxel size of $0.47 \times 0.47 \times 0.47$ mm^3 and the VOI with $512 \times 512 \times 512$ voxels with a voxel size of $0.1 \times 0.1 \times 0.1$ mm^3.

Reference Scan. For reference, an HD scan was executed. Because no standard protocols were available for FPCT imaging of the inner ear, we used a protocol recently investigated for this application.[15] Four hundred ninety-six projections with a 2×2 pixel binning were acquired. The lateral collimation was completely opened to enable the maximal SFOV of 240 mm in diameter. The collimation in the z-direction was narrowed to get an exposed length of 60 mm as in the MSCT protocol. The tube voltage was set to 70 kV, and the DED, to 3.60 μGy/projection.

MSCT Scanning

Because MSCT constitutes the state-of-the-art technique for inner ear investigations, an MSCT scan with the CT system Somatom Definition Flash (Siemens) was obtained for reference. We used the standard application, the inner ear high-resolution protocol, as proposed by the manufacturer. The tube voltage was 120 kV, the tube current-time product was 180 mAs, the pitch was 0.85 mm, the collimation was 16×0.6 mm, and the scan length was 60 mm. At the workstation of the scanner, a volume with an image matrix of 512×512 pixels of 0.1×0.1 mm^2 pixel size and 0.6-mm-thick sections of 0.3 mm increment was reconstructed by using a sharp reconstruction kernel (U75u).

Monte Carlo Dose Simulations

3D dose distributions were calculated with the Monte Carlo tool ImpactMC (CT Imaging, Erlangen, Germany), which was validated for patient-specific dose simulations recently.[19,20] Spatial dose distributions for the OV, VOI, HD, and MSCT scans were simulated sepa-
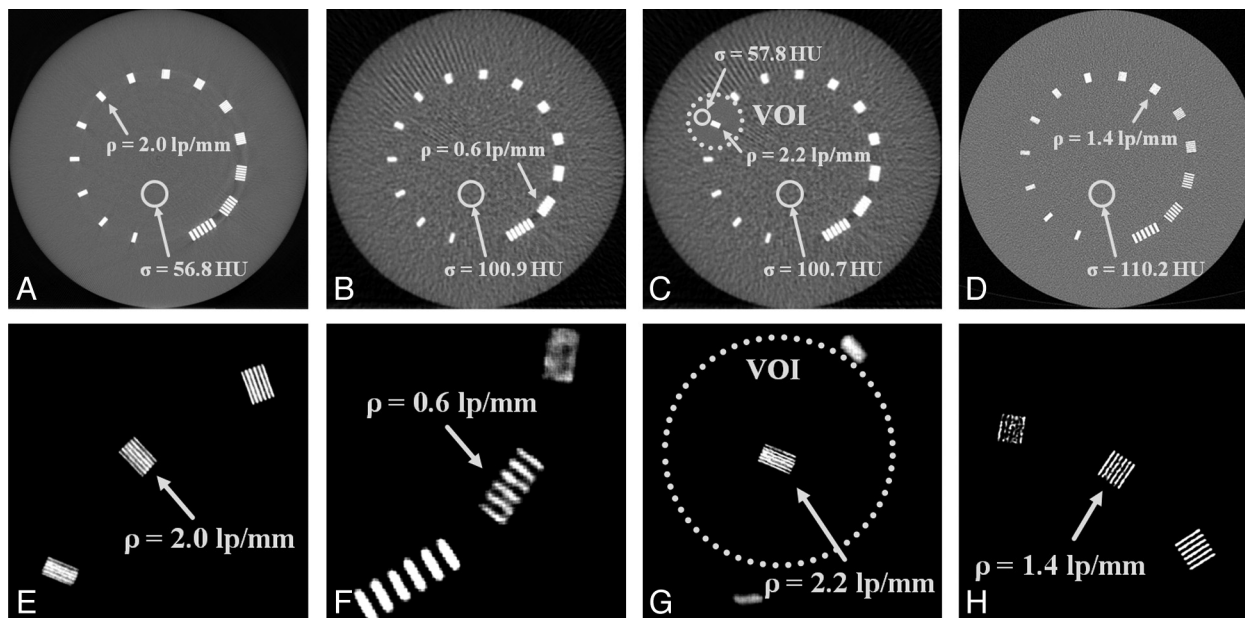
Fig 2. Measurements of a bar pattern phantom to determine spatial resolution (ρ) and image noise (σ). *A–D*, Complete images of the phantom (center = 0 HU, width = 1000 HU). *E–H*, Detailed images of the respective resolution bar pattern (center = 1000 HU, width = 500 HU) for the HD scan (*A* and *E*), the OV scan (*B* and *F*), the combination of OV and VOI scans (*C* and *G*), and the MSCT scan (*D* and *H*).

rately by using the given scan parameters (eg, the source and detector trajectories and collimation settings). All FPCT dose distributions were computed for 70 kV and scaled by the kerma free-in-air value of 6.2 mGy/100 mAs on the axis of rotation,[19,20] measured by using a calibrated ionization chamber. For the MSCT dose distribution, 120 kV tube voltage and the air kerma value of 16.3 mGy/100 mAs were used. The dose of the proposed 2-scan procedure (OV and VOI) was compared with that obtained for the HD and MSCT scans. For this, the absorbed dose in the head was derived by calculating the mean values in the head region of the simulated 3D dose distributions.

Results

Image-Quality Results
The VOI, in our case the relevant bar pattern and the inner ear, could easily be selected in the OV volume despite the limited image quality (Figs 2 and 3). The fine structures were blurred in the OV scan but could be recognized. Spatial resolution was 0.6 lp/mm, and image noise, 101 HU (Fig 2). Performance parameters are summarized in the Table. In the combined images of OV and VOI scans, the bone structures within the VOIs (eg, the stapes and the cochlea) were sharply delimited. This was ensured by the smaller pixel size and higher dose, resulting in a spatial resolution of 2.2 lp/mm and image noise of 58 HU. In comparison with the HD scan with a spatial resolution of 2.0 lp/mm and an image noise of 57 HU, the resolution within the VOI was slightly higher. This was due to positioning the structure of interest in the rotation center of the VOI scan where angular sampling is higher than that in the periphery. In comparison with the MSCT scan with a spatial resolution of 1.4 lp/mm and image noise of 110 HU, both the VOI scan and the HD scan provided higher image quality (Fig 3).

Dose Results
The 3D dose distributions obtained by Monte Carlo simulations are shown in Fig 4 and are summarized in the Table. The

proposed 2-scan procedure reduced the dose significantly compared with a full HD scan as well as with an MSCT scan. Especially areas outside the VOI exhibited a significantly reduced dose level; inside the VOI, the dose level was also decreased. The highest dose was applied by the HD scan, followed by the MSCT scan, and the VOI approach using the lowest dose. The cumulative dose for the combined VOI approach of 1.6 mGy resulted from 0.2 mGy for the low-dose OV scan and 1.4 mGy for the local HD VOI scan. The dose was 14.7 mGy in the HD scan and 8.2 mGy in the MSCT scan. In comparison with the HD scan with full SFOV and comparable image quality, the VOI allowed a dose reduction of 90%. In comparison with the MSCT scan, the state-of-the-art protocol for inner ear investigations, the VOI was imaged at higher quality, yet with the dose reduced by 82.6%.

Discussion
The data and results presented in this article show the technical feasibility and the benefits of VOI imaging. The possibilities for improvement of image quality for a limited VOI and, at the same time, for a reduction of total dose are realistic and appear very promising. Yet, technical and practical aspects have to be taken into account.

It is desirable to perform the combined examination without moving the patient. This apparently is possible by using the advantages of a robot-driven C-arm system. Unfortunately, our system did not allow changing the focus-isocenter distance, which forced us to work with a constant magnification for the OV and VOI scan. With increased magnification, higher spatial resolution would certainly be achieved as was shown by simulations.[11,18]

Concerning the data and workflow, the advanced method presented here improved the data acquisition and the data combination of the OV and VOI scans. The C-arm is moved to the VOI isocenter by the robot system between the 2 scans. The
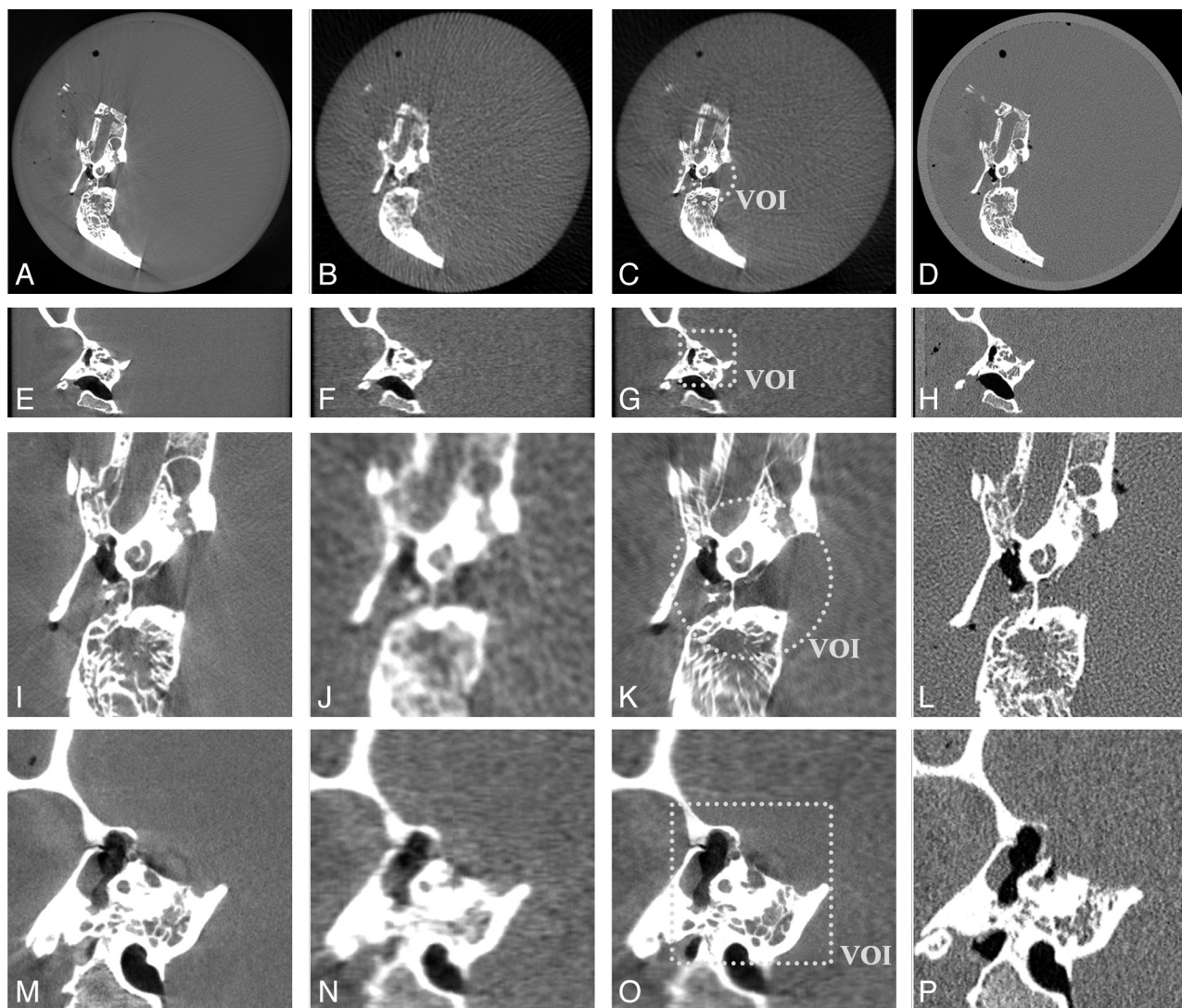
Fig 3. Measurements of an inner ear specimen. Complete transversal views (A–D), complete coronal views (E–H), detailed transversal views (I–L), and detailed coronal views (M–P). The first column shows the HD scan; the second column, the OV scan; the third column, the combination of the OV and VOI scans; and the last column, the MSCT scan (center = 0 HU, width = 2000 HU).

Summary of spatial resolution, image noise, and dose values			
Scan	Spatial Resolution (lp/mm)	Image Noise (HU)	Dose (mGy)
OV	0.6	101	0.2
VOI	2.2	58	1.4
OV + VOI	2.2	58	1.6
HD	2.0	57	14.7
MSCT	1.4	110	8.2

patient does not have to be moved, and the C-arm can automatically be aligned to the VOI. Another improvement shown by this investigation is the direct use of the C-arm coordinates provided by the robot. Thus external registration (eg, image- or camera-based) was no longer necessary, which facilitated the combination procedure. Both advances make the VOI approach time-efficient, stable, and user-friendly, which should help with respect to the clinical applicability of this imaging approach.

Possible medical applications are not limited to the imaging of the human inner ear (eg, for the diagnostic evaluation of

implants). Interventional CT and dynamic CT are prime candidates. Any type of repeated scanning of a limited region (eg, a lesion that has previously been identified) can be performed at a reduced dose. The degree to which the dose is reduced will depend, of course, on selecting a small VOI. Respective clinical experience is not yet available.

In comparison with HD modes in FPCT and with standard MSCT, the VOI approach has the potential to provide better image quality with higher spatial resolution and lower image noise when focusing only on a VOI.

Conclusions

Standard FPCT protocols enable imaging of the inner ear.[15] Improving FPCT with the proposed VOI approach can ensure higher image quality while simultaneously reducing the cumulative dose significantly. Even in comparison with MSCT, image quality was improved for the VOI and the total dose was reduced significantly. These improvements indicate that FPCT imaging may become an important technique in diagnostic imaging of the human inner ear as
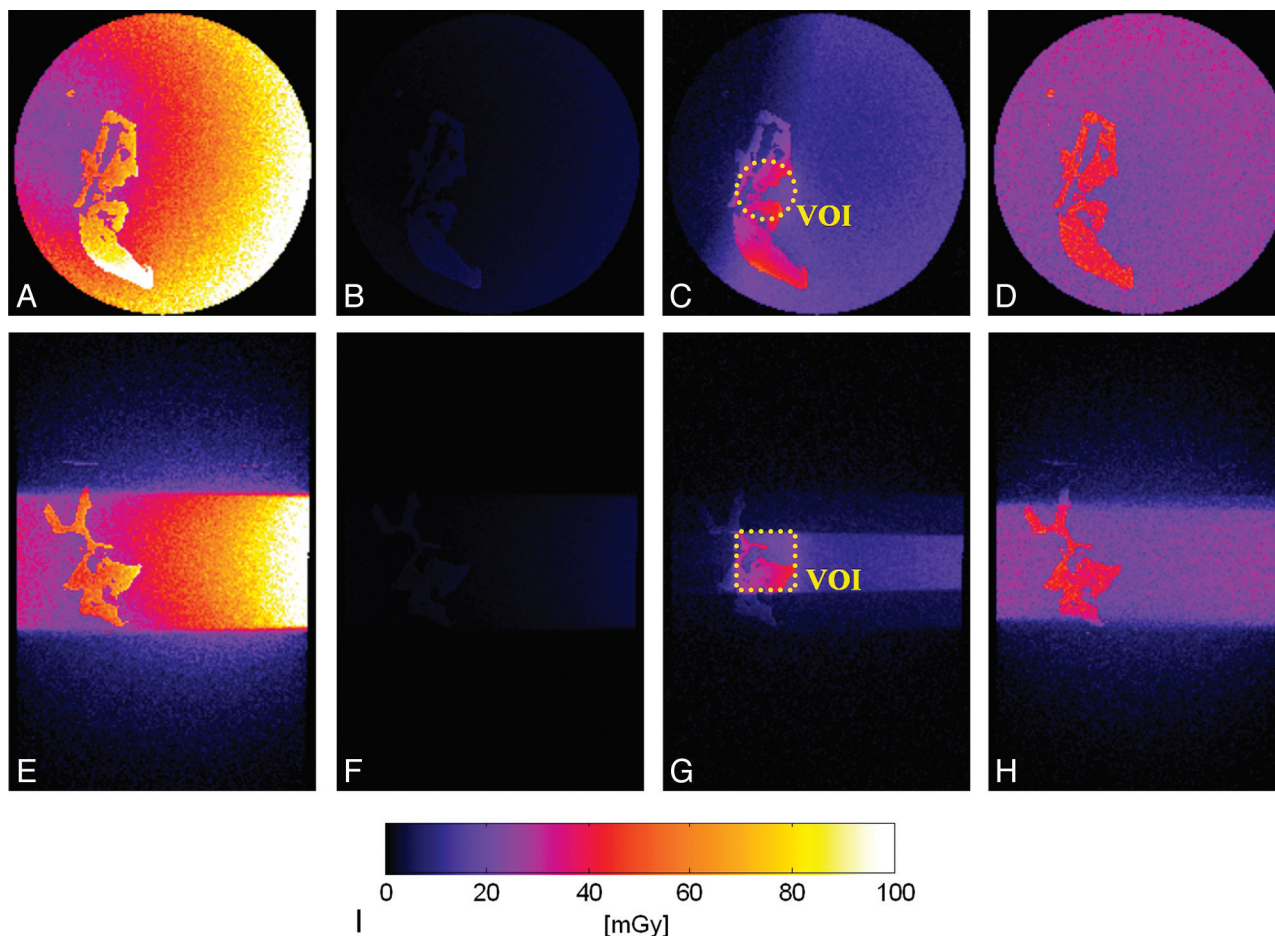
Fig 4. Monte Carlo dose simulations for the different scanning approaches in transversal (*A–D*) and coronal views (*E–H*) for the HD scan (*A* and *E*), the OV scan (*B* and *F*), the combination of OV and VOI scans (*C* and *G*), and the MSCT scan (*D* and *H*). All distributions are scaled according to the color scale shown in *I*.

soon as appropriate implementations are made available by the manufacturers.

Disclosures: Willi A. Kalendar, *Consultant*: Siemens, Healthcare Sector.

References

1. Chun IK, Cho MH, Lee SC, et al. **X-ray micro-tomography system for small-animal imaging with zoom-in imaging capability.** *Phys Med Biol* 2004;49:3889–902
2. Chityala R, Hoffmann KR, Rudin S, et al. **Region of interest (ROI) computed tomography (CT): comparison with full field of view (FFOV) and truncated CT for a human head phantom.** *Proc SPIE* 2005;5745:583–90
3. Cho S, Bian J, Pelizzari CA, et al. **Region-of-interest image reconstruction in circular cone-beam microCT.** *Med Phys* 2007;34:4923–33
4. Chen L, Shaw CC, Altunbas MC, et al. **Feasibility of volume-of-interest (VOI) scanning technique in cone beam breast CT: a preliminary study.** *Med Phys* 2008;35:3482–90
5. Patel V, Hoffmann KR, Ionita CN, et al. **Rotational micro-CT using a clinical C-arm angiography gantry.** *Med Phys* 2008;35:4757–64
6. Cho S, Pearson E, Pelizzari CA, et al. **Region-of-interest image reconstruction with intensity weighting in circular cone-beam CT for image-guided radiation therapy.** *Med Phys* 2009;36:1184–92
7. Chen L, Shen Y, Lai C-J, et al. **Dual resolution cone beam breast CT: a feasibility study.** *Med Phys* 2009;36:4007–14
8. Lai C-J, Chen L, Zhang H, et al. **Reduction in x-ray scatter and radiation dose for volume-of-interest (VOI) cone-beam breast CT: a phantom study.** *Phys Med Biol* 2009;54:6691–709
9. Yu H, Wang G. **Compressed sensing based interior tomography.** *Phys Med Biol* 2009;54:2791–805
10. Schafer S, Noël PB, Walczak AM, et al. **Filtered region of interest cone-beam rotational angiography.** *Med Phys* 2010;37:694–703
11. Kolditz D, Kyriakou Y, Kalender WA. **Volume-of-interest (VOI) imaging in C-arm flat-detector CT for high image quality at reduced dose.** *Med Phys* 2010;37:2719–30
12. Kalender WA, inventor; Method for recording images of a definable region of an examination object using a computed tomography facility. US patent US 2008/0075225, Siemens AG, March 27, 2008
13. Kalender WA, inventor; Verfahren zur Aufnahme von Bildern eines bestimmbaren Bereichs eines Untersuchungsobjekts mittels einer Computerto-mographieeinrichtung. German patent DE 10 2006 044 783.03, Siemens AG and University of Erlangen-Nürnberg, April 3, 2008
14. Bozzato A, Struffert T, Hertel V, et al. **Analysis of the accuracy of high-resolution computed tomography techniques for the measurement of stapes prostheses.** *Eur Radiol* 2010;20:566–71
15. Struffert T, Hertel V, Kyriakou Y, et al. **Imaging of cochlear implant electrode array with flat-detector CT and conventional multislice CT: comparison of image quality and radiation dose.** *Acta Otolaryngol* 2010;130:443–52
16. Feldkamp LA, Davis LC, Kress JW. **Practical cone-beam algorithm.** *J Opt Soc Am A* 1984;1:612–19
17. Kalender WA, Kyriakou Y. **Flat-detector computed tomography (FD-CT).** *Eur Radiol* 2007;17:2767–79
18. Kolditz D, Kyriakou Y, Kalender WA. **Low dose, low noise and high resolution volume of interest (VOI) imaging in C-arm flat-detector CT.** *Proc SPIE* 2010;7622:26
19. Deak P, van Straten M, Shrimpton PC, et al. **Validation of a Monte Carlo tool for patient-specific dose simulations in multi-slice computed tomography.** *Eur Radiol* 2008;18:759–72
20. Kyriakou Y, Deak P, Langner O, et al. **Concepts for dose determination in flat-detector CT.** *Phys Med Biol* 2008;53:3551–66